Inorganic Chemistry

Article

Rhenium Analogues of Promising Renal Imaging Agents with a {^{99m}Tc(CO)$_3$}$^+$ Core Bound to Cysteine-Derived Dipeptides, Including Lanthionine

Haiyang He,[†] Malgorzata Lipowska,[†] Xiaolong Xu,[†] Andrew T. Taylor,[†] and Luigi G. Marzilli*,[‡]

Department of Radiology, Emory University, Atlanta, Georgia 30322, and Department of Chemistry, Louisiana State University, Baton Rouge, Louisiana 70803

The coordination chemistry of lanthionine (LANH$_2$) and cystathionine (CSTH$_2$) dipeptides, which respectively consist of two cysteines and one cysteine and one homocysteine linked by a thioether bridge, is almost unstudied. Recently for *fac*-[^{99m}Tc(CO)$_3$(LAN)]$^-$ isomers, the first small ^{99m}Tc(CO)$_3$ agents evaluated in humans were found to give excellent renal images and to have a high specificity for renal excretion. Herein we report the synthesis and characterization of Re complexes useful for interpreting the nature of tracer ^{99m}Tc radiopharmaceuticals. Treatment of [Re(CO)$_3$(H$_2$O)$_3$]OTf with commercially available LANH$_2$ (a mixture of meso (D,L) and chiral (DD,LL) isomers) gave three HPLC peaks, **1A**, **1B**, and **1C**, but treatment with CSTH$_2$ (L,L isomer) gave one major product, Re(CO)$_3$-(CSTH) (**2**). Crystalline Re(CO)$_3$(LANH) products were best obtained with synthetic LANH$_2$, richer in meso or chiral isomers. X-ray crystallography showed that these dipeptides coordinate as tridentate N$_2$S-bound ligands with two dangling carboxyls. The LANH ligand is meso in **1A** and **1C** and chiral in **1B**. While **1A** (kinetically favored) is stable at ambient temperature for days, it converted into **1C** (thermodynamically favored) at 100 °C; after 6 h, equilibrium was reached at a **1A**:**1C** ratio of 1:2 at pH 8. The structures provide a rationale for this behavior and for the fact that **1A** and **1C** have simple NMR spectra. This simplicity results from fluxional interchange between an enantiomer with both chelate rings having the same δ pucker and an enantiomer with both chelate rings having the same λ pucker. Agents with the {^{99m}Tc(CO)$_3$}$^+$ core and N$_2$S ligands show promise of becoming an important class of ^{99m}Tc radiopharmaceuticals. The chemistry of Re analogues with these ligands, such as the LAN^{2-} complexes reported here, provides a useful background for designing new small agents and also tagged large agents because two uncoordinated carboxyl groups are available for conjugation with biological molecules such as proteins.

Introduction

In a search for superior ^{99m}Tc renal imaging agents,[1–3] we have been exploring possible radiopharmaceuticals containing a {^{99m}Tc(CO)$_3$}$^+$ core.[4–6] [^{99m}Tc(CO)$_3$(H$_2$O)$_3$]$^+$, the precursor used to radiolabel biomolecules with this core,

can be prepared in aqueous solution, and it is stable over a wide pH range.[7,8] The aqua ligands of the [^{99m}Tc(CO)$_3$-(H$_2$O)$_3$]$^+$ precursor are readily substituted by ligands possessing a variety of ligating groups. The chemically robust {^{99m}Tc(CO)$_3$}$^+$ core provides a convenient platform for the development of radiopharmaceuticals.[9–14]

* To whom correspondence should be addressed. E-mail: lmarzil@lsu.edu.
† Emory University.
‡ Louisiana State University.

(1) Eshima, D.; Eshima, L.; Hansen, L.; Lipowska, M.; Marzilli, L. G.; Taylor, A. *J. Nucl. Med.* **2000**, *41*, 2077–2082.
(2) Taylor, A.; Hansen, L.; Eshima, D.; Malveaux, E.; Folks, R.; Shattuck, L.; Lipowska, M.; Marzilli, L. G. *J. Nucl. Med.* **1997**, *38*, 821–826.
(3) Lipowska, M.; Hansen, L.; Xu, X.; Marzilli, P. A.; Taylor, A.; Marzilli, L. G. *Inorg. Chem.* **2002**, *41*, 3032–3041.
(4) Lipowska, M.; Cini, R.; Tamasi, G.; Xu, X.; Taylor, A. T.; Marzilli, L. G. *Inorg. Chem.* **2004**, *43*, 7774–7783.
(5) Lipowska, M.; He, H.; Malveaux, E.; Xu, X.; Marzilli, L. G.; Taylor, A. *J. Nucl. Med.* **2004**, *45*, 461P.
(6) He, H.; Lipowska, M.; Xu, X.; Taylor, A. T.; Carlone, M.; Marzilli, L. G. *Inorg. Chem.* **2005**, *44*, 5437–5446.
(7) Alberto, R.; Ortner, K.; Wheatley, N.; Schibli, R.; Schubiger, A. P. *J. Am. Chem. Soc.* **2001**, *123*, 3135–3136.
(8) Alberto, R.; Schibli, R.; Egli, A.; Schubiger, A. P. *J. Am. Chem. Soc.* **1998**, *120*, 7987–7988.
(9) Muller, C.; Schubiger, P. A.; Schibli, R. *Bioconjugate Chem.* **2006**, *17*, 797–806.
(10) James, S.; Maresca, K. P.; Allis, D. G.; Valliant, J. F.; Eckelman, W.; Babich, J. W.; Zubieta, J. *Bioconjugate Chem.* **2006**, *17*, 579–589.
(11) James, S.; Maresca, K.; Babich, J.; Valliant, J.; Doering, L.; Zubieta, J. *Bioconjugate Chem.* **2006**, *17*, 590–596.

Pharmacokinetics and biodistribution studies on ^{99m}Tc-$(CO)_3$ agents have shown that agents with tridentate ligands exhibit better clearance characteristics in vivo than agents with mono- or bidentate ligands.[15] Past studies on the biocoordination chemistry of the $\{^{99m}M(CO)_3\}^+$ core (M=Tc, Re) have revealed that ligands with thioether or aromatic sp^2 nitrogen donors form complexes most readily.[16−20] Important characteristics of superior ^{99m}Tc renal imaging agents include high specificity for renal excretion and rapid clearance from the bloodstream.[21−29] Toward this end, highly hydrophilic agents are necessary. ^{99m}Tc agents designed to target the organic anion tubular transporter generally have high clearance.[2,30−32] Because a carboxyl group is important in order for molecules to have an efficient interaction with the renal tubular transporter, an uncoordinated carboxyl group is a desirable feature for ligands in renal imaging agents.[31]

Peptides can meet these ligand requirements; moreover, peptides can tolerate the harsh conditions sometimes needed for chemical modification or radiolabeling. Furthermore, compared to other ligand types, small peptides form agents that are less likely to be immunogenic and more likely to have rapid blood clearance. ^{99m}Tc-labeled peptides have emerged as an important class of radiopharmaceuticals in diagnostic nuclear medicine.[33] Integration of pyridyl ligating

Chart 1
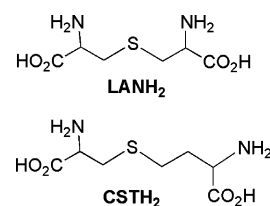
groups into amino acids or peptides enhances the efficiency of labeling these molecules with the $\{^{99m}Tc(CO)_3\}^+$ core.[34,35] However, agents with lipophilic pyridine rings usually have undesirably high hepatobiliary uptake.[36] In our past studies we showed that S-propyl-L-cysteine ligands form rhenium tricarbonyl complexes by binding through both thioether and amino groups.[6] Peptides derived from cysteine can provide sulfur donors to act with amine and carboxyl donors for favorable coordination to the $\{^{99m}Tc(CO)_3\}^+$ core, and such peptides lack lipophilic groups. We now employ this strategy with S-dipeptides with the two amino acids linked by a thioether bridge rather than by a peptide bond. By avoiding a peptide link, the carboxyl group is free to interact with the renal tubular transporter. In addition, because the central S anchors the tridentate ligand, carboxyl oxygen binding would lead to less favorable larger chelate rings. Thus, NOS binding is less favored than N_2S binding by the S-dipeptides. The two amino acids linked by a shared sulfur are cysteine in lanthionine (LANH$_2$) and L-cysteine and L-homocysteine in cystathionine (CSTH$_2$) (cf. Chart 1).

We selected these small monosulfide-bridged S-dipeptides because they are more stable than the labile disulfide-bridged dipeptides such as cystine.[37] We expected these ligands to bind as dianions (LAN$^{2−}$ and CST$^{2−}$), forming ^{99m}Tc(I)(CO)$_3$ agents that are monoanions at physiological pH. In general, good renal agents are anions of low charge.[31] Recently we evaluated [^{99m}Tc(CO)$_3$(LAN)]$^−$ agents in humans;[38] this was only the second report of a human study of agents based on the $\{^{99m}Tc(CO)_3\}^+$ core and the first report of a human study with $\{^{99m}Tc(CO)_3\}^+$ core-containing small agents, in this case, renal imaging agents.[38] The [^{99m}Tc(CO)$_3$(LAN)]$^−$ agents gave excellent renal images and had a high specificity for renal excretion. Nonradioactive Re analogues are useful for understanding the chemistry of the radioactive ^{99m}Tc species and in guiding ligand design. This analogue approach has been used widely to develop and to evaluate radiopharmaceutical agents with the $\{^{99m}Tc(V)O\}^{3+}$ core.[22,39,40] Here we

(12) Karagiorgou, O.; Patsis, G.; Pelecanou, M.; Raptopoulou, C. P.; Terzis, A.; Siatra-Papastaikoudi, T.; Alberto, R.; Pirmettis, I.; Papadopoulos, M. *Inorg. Chem.* **2005**, *44*, 4118−4120.
(13) Haefliger, P.; Agorastos, N.; Renard, A.; Giambonini-Brugnoli, G.; Marty, C.; Alberto, R. *Bioconjugate Chem.* **2005**, *16*, 582−587.
(14) Schibli, R.; Dumas, C.; Petrig, J.; Spadola, L.; Scapozza, L.; Garcia-Garayoa, E.; Schubiger, P. A. *Bioconjugate Chem.* **2005**, *16*, 105−112.
(15) Schibli, R.; La Bella, R.; Alberto, R.; Garcia-Garayoa, E.; Ortner, K.; Abram, U.; Schubiger, P. A. *Bioconjugate Chem.* **2000**, *11*, 345−351.
(16) Lazarova, N.; Babich, J.; Valliant, J.; Schaffer, P.; James, S.; Zubieta, J. *Inorg. Chem.* **2005**, *44*, 6763−6770.
(17) Pietzsch, H. J.; Gupta, A.; Reisgys, M.; Drews, A.; Seifert, S.; Syhre, R.; Spies, H.; Alberto, R.; Abram, U.; Schubiger, P. A.; Johannsen, B. *Bioconjugate Chem.* **2000**, *11*, 414−424.
(18) Wust, F.; Skaddan, M. B.; Leibnitz, P.; Spies, H.; Katzenellenbogen, J.; Johannsen, B. *Bioorg. Med. Chem.* **1999**, *7*, 1827−1835.
(19) Santos, I. G.; Abram, U.; Alberto, R.; Lopez, E. V.; Sanchez, A. *Inorg. Chem.* **2004**, *43*, 1834−1836.
(20) Alves, S.; Paulo, A.; Correia, J. D. G.; Domingos, A.; Santos, I. *J. Chem. Soc., Dalton Trans.* **2002**, 4714−4719.
(21) Lipowska, M.; Hansen, L.; Marzilli, L. G.; Taylor, A. *J. Nucl. Med.* **2001**, *42*, 259P.
(22) Hansen, L.; Marzilli, L. G.; Taylor, A. *J. Nucl. Med.* **1998**, *42*, 280−293.
(23) Hansen, L.; Hirota, S.; Xu, X.; Taylor, A.; Marzilli, L. G. *Inorg. Chem.* **2000**, *39*, 5731−5740.
(24) Hansen, L.; Lipowska, M.; Melendez, E.; Xu, X.; Hirota, S.; Taylor, A.; Marzilli, L. G. *Inorg. Chem.* **1999**, *38*, 5351−5358.
(25) Hansen, L.; Yue, K. T.; Xu, X.; Lipowska, M.; Taylor, A., Jr.; Marzilli, L. G. *J. Am. Chem. Soc.* **1997**, *38*, 8965−8972.
(26) Hansen, L.; Xu, X.; Yue, K. T.; Kuklenyik, Z.; Taylor, A.; Marzilli, L. G. *Inorg. Chem.* **1996**, *35*, 1958−1966.
(27) Hansen, L.; Lipowska, M.; Taylor, A.; Marzilli, L. G. *Inorg. Chem.* **1995**, *34*, 3579−3580.
(28) Marzilli, L. G.; Banaszczyk, M. G.; Hansen, L.; Kuklenyik, Z.; Cini, R.; Taylor, A., Jr. *Inorg. Chem.* **1994**, *33*, 4850−4860.
(29) Hansen, L.; Cini, R.; Taylor, A.; Marzilli, L. G. *Inorg. Chem.* **1992**, *31*, 2801−2808.
(30) Taylor, A.; Eshima, D.; Fritzberg, A. R.; Christian, P. E. *J. Nucl. Med.* **1986**, *27*, 795−803.
(31) Shikano, S.; Kanai, Y.; Kawai, K.; Ishikawa, N.; Endou, H. *J. Nucl. Med.* **2004**, *45*, 80−85.
(32) Fritzberg, A. R.; Kasina, S.; Eshima, D.; Johnson, D. L. *J. Nucl. Med.* **1986**, *27*, 111−116.
(33) Liu, S.; Edwards, D. S. *Chem. Rev.* **1999**, *99*, 2235−2268.
(34) Stephenson, K. A.; Banerjee, S. R.; Sogbein, O. O.; Levadala, M. K.; McFarlane, N.; Boreham, D. R.; Maresca, K. P.; Babich, J. W.; Zubieta, J.; Valliant, J. F. *Bioconjugate Chem.* **2005**, *16*, 1189−1195.
(35) Banerjee, S. R.; Levadala, M. K.; Lazarova, N.; Wei, L.; Valliant, J. F.; Stephenson, K. A.; Babich, J. W.; Maresca, K. P.; Zubieta, J. *Inorg. Chem.* **2002**, *41*, 6417−6425.
(36) Vanbilloen, H. P.; Bormans, G. M.; Deroo, M. J.; Verbruggen, A. M. *Nucl. Med. Biol.* **1995**, *22*, 325−338.
(37) Swali, V.; Matteucci, M.; Elliot, R.; Bradley, M. *Tetrahedron* **2002**, *58*, 9101−9109.
(38) Lipowska, M.; He, H.; Malveaux, E.; Xu, X.; Marzilli, L. G.; Taylor, A. *J. Nucl. Med.* **2006**, *47*, 1032−1040.
(39) Wong, E.; Bennett, S.; Lawrence, B.; Fauconnier, T.; Lu, L. F. L.; Bell, R. A.; Thornback, J. R.; Eshima, D. *Inorg. Chem.* **2001**, *40*, 5695−5700.
(40) DiZio, J. P.; Fiaschi, R.; Davison, A.; Jones, A, G.; Katzenellenbogen, J. A. *Bioconjugate Chem.* **1991**, *2*, 353−366.

report the chemistry of Re(CO)$_3$ complexes made with LANH$_2$ and CSTH$_2$.

Lanthionine, a naturally occurring S-dipeptide, was first detected in 1941 in alkaline hydrolysates of wool.[41] Lanthionines also occur naturally in certain peptide and protein antibiotics and in body organs and tissues, where their formation may be a function of the aging process. LANH$_2$ has been found in several biologically important compounds.[42] Considerable effort has been devoted toward incorporating LANH$_2$ into peptides and proteins that possess promising biomedical application.[43,44] Lanthionine is a key component of the lantibiotics, a family of antimicrobial peptides such as nisin, duramycin, and subtilin produced by Gram-positive bacteria. Many of these peptides show potent antibiotic properties; others are believed to act as enzyme inhibitors.[37,45−48] Structure−activity relationships for a series of cyclic somatostatin analogues containing a lanthionine bridge, such as sandostatin, have revealed that the introduction of a lanthionine bridge significantly increased receptor binding selectivity.[49−51]

In summary, both LANH$_2$ and CSTH$_2$ have important biological activities.[52] From the structures, these molecules should still behave as chelating ligands. However, until this report, no isolated well-characterized metal complexes of these S-dipeptides have been reported in the literature. Also, the LANH$_2$ isomers are difficult to differentiate, and the synthesis of complexes reveals that commercially available LANH$_2$ is a mixture, complicating the synthesis of complexes. In this work, we evaluate some of the organic synthetic schemes that have been suggested in the literature to produce isomerically pure LANH$_2$.

Experimental Section

General Methods. All reagents and organic solvents were reagent grade and were used without further purification. L-Cystathionine was purchased from Sigma-Aldrich; lanthionine was purchased from TCI America and used as received. Because commercially available lanthionine was a mixture of meso (D,L) and chiral (D,D and L,L) isomers, it was also synthesized by a published method (see below).[53] [Re(CO)$_3$(H$_2$O)$_3$]OTf, prepared by

(41) Brown, G.; Du Vigneaud, V. *J. Biol. Chem.* **1941**, *140*, 767−771.
(42) O'Keefe, B. R. *J. Nat. Prod.* **2001**, *64*, 1373−1381.
(43) Chatterjee, C.; Paul, M.; Xie, L.; vanderDonk, W. A. *Chem. Rev.* **2005**, *105*, 633−684.
(44) Patton, G. C.; van der Donk, W. A. *Curr. Opin. Microbiol.* **2005**, *8*, 543−551.
(45) Seyberth, T.; Voss, S.; Brock, R.; Wiesmüller, K.-H.; Jung, G. *J. Med. Chem.* **2006**, *49*, 1754−1765.
(46) Mustapa, M. F. M.; Harris, R.; Bulic-Subanovic, N.; Elliott, S.; Bregant, S.; Groussier, M. F. A.; Mould, J.; Schultz, D.; Chubb, N. A. L.; Gaffney, P. R. J.; Driscoll, P. C.; Tabor, A. B. *J. Org. Chem.* **2003**, *68*, 81858192.
(47) Li, J. T.; Kiang, X. H.; Goodman, M. *J. Pept. Sci.* **2001**, *7*, 82−91.
(48) Dugave, C.; Nenez, A. *Tetrahedron: Asymmetry* **1997**, *8*, 1453−1465.
(49) Osapay, G.; Prokai, L.; Kim, H. S.; Medzihradszky, K. F.; Coy, D. H.; Liapakis, G.; Reisine, T.; Melacini, G.; Zhu, Q.; Wang, S. H. H.; Mattern, R. H.; Goodman, M. *J. Med. Chem.* **1997**, *40*, 2241−2251.
(50) Gademann, K.; Kimmerlin, T.; Hoyer, D.; Seebach, D. *J. Med. Chem.* **2001**, *44*, 2460−2468.
(51) Sukopp, M.; Schwab, R.; Marinelli, L.; Biron, E.; Heller, M.; Varkondi, E.; Pap, A.; Novellino, E.; Keri, G.; Kessler, H. *J. Med. Chem.* **2005**, *48*, 2916−2926.
(52) Wirtz, M.; Droux, M. *Photosynth. Res.* **2005**, *86*, 345−362.
(53) Harpp, D. N.; Gleason, J. G. *J. Org. Chem.* **1971**, *36*, 73−80.

the method we previously reported,[6] was stored and used as a 0.1 M stock aqueous solution. ^{1}H NMR spectra were recorded on a Varian 400 or 600 MHz spectrometer; chemical shifts were referenced to internal sodium 3-(trimethylsilyl)propionate-d_4 (TSP, 0.00 ppm) in D$_2$O and the solvent peak in DMSO-d_6 (2.48 ppm). HPLC analyses were performed on a Waters Breeze system equipped with a Waters 2487 dual wavelength absorbance detector, Waters 1525 binary pump, and XTerra MS C18 column (5 μm; 4.6 × 250 mm). HPLC solvents consisted of the buffer [0.05 M TEAP (aqueous triethylammonium phosphate) at pH 2.5, solvent A] and methanol (solvent B). The HPLC system started with 100% of A from 0 to 3 min. The eluent switched at 3 min to 75% A/25% B, at 6 min to 66% A/34% B, and remained for 3 more min, followed by linear gradients: 66% A/34% B to 34% A/66% B from 9 to 20 min and 34% A/66% B to 100% A from 20 to 30 min. The flow rate was 1 mL/min. Elemental analyses were performed by Atlantic Microlabs, Atlanta, GA.

Re(CO)$_3$(LANH). A stirred suspension of LANH$_2$ (predominantly meso, 0.101 g, 0.5 mmol), [Re(CO)$_3$(H$_2$O)$_3$]OTf (5 mL, 0.5 mmol), and 15 mL of water at 75 °C was treated slowly with 0.1 M NaOH to maintain the pH at 8. The clear solution that formed after 20 min was stirred at 75 °C for 40 min. HPLC analysis of the solution showed three peaks with retention times (RT) of 10.8 (**1A**), 9.9 (**1B**), and 8.8 min (**1C**) in a 7:1.5:1.5 ratio. The solution was concentrated to 2−3 mL by rotary evaporation and desalted on a Sephadex G-15 column (eluted with deionized water). The product fractions collected were reduced to 5 mL and acidified with HCl to pH 3. Product **1A** deposited when the solution was left overnight at ambient temperature; yield, 0.13 g (54%). The above preparative procedure starting with the commercially available mixture of LANH$_2$ isomers gave **1A**, **1B**, and **1C** in a ratio of 5:4:1. Pure **1B** was obtained by preparative HPLC.

Conversion of 1A into 1C. A solution of **1A** (0.12 g) in water (25 mL) at pH 8 was stirred under reflux conditions. The conversion of **1A** into **1C** was monitored by HPLC. At 6 h, **1C** was present as the major product (**1C**:**1A** = 2:1). Pure **1C** was obtained via preparative HPLC.

1A. Anal. Calcd for C$_9$H$_{11}$N$_2$O$_7$SRe: C, 22.64; H, 2.32; N, 5.87; S, 6.72. Found: C, 22.59; H, 2.54; N, 5.80; S, 6.55. ^{1}H NMR [δ (ppm), D$_2$O, pH ∼11]: 3.68 (dd, 2H, Hα, J = 7.8 and 6.6 Hz), 3.27 (dd, 2H, Hβ, J = 14.4 and 6.6 Hz) and 3.07 (dd, 2H, Hβ, J = 14.4 and 7.8 Hz).

1B. Anal. Calcd for C$_9$H$_{11}$N$_2$O$_7$SRe·H$_2$O: C, 21.82; H, 2.64; N, 5.65; S, 6.47. Found: C, 21.90; H, 2.58; N, 5.70; S, 6.47. ^{1}H NMR data are described in results.

1C. Anal. Calcd for C$_9$H$_{11}$N$_2$O$_7$SRe·1.5H$_2$O: C, 21.43; H, 2.80; N, 5.55; S, 6.36. Found: C, 21.52; H, 2.89; N, 5.54; S, 6.38. ^{1}H NMR [δ (ppm), D$_2$O, pH ∼11]: 3.73 (dd, 2H, Hα, J = 8.0 and 5.2 Hz), 3.16 (dd, 2H, Hβ, J = 14.2 and 8.0 Hz) and 3.07 (dd, 2H, Hβ, J = 14.2 and 5.2 Hz).

Re(CO)$_3$(CSTH) (2). A stirred suspension of CSTH$_2$ (0.066 g, 0.3 mmol), [Re(CO)$_3$(H$_2$O)$_3$]OTf (3 mL, 0.3 mmol), and 10 mL of water at 75 °C was treated slowly with 0.1 M NaOH to maintain the pH at 8. The clear solution that formed after 10 min was stirred at 75 °C for 40 min, then acidified (HCl) to pH 3, concentrated to 3 mL, and left to stand overnight at ambient temperature to give **2** (0.065 g, 44% yield). Anal. Calcd for C$_{10}$H$_{13}$N$_2$O$_7$SRe: C, 22.44; H, 2.67; N, 5.70; S, 6.52. Found: C, 22.16; H, 3.00; N, 5.57; S, 6.24. ^{1}H NMR [δ (ppm)]: 4.10 (dd, 1H), 3.36−3.07 (m, 5H), 2.46 (dd, 1H) and 2.08 (m, 1H). Interpretation of the spectrum recorded in D$_2$O, pH ∼11 is challenging because of the overlap of two signals between 3.3 and 3.4 ppm and the partial overlap of a signal at 3.2 ppm. Signals at 4.10 (Hα, J = 5 and 6 Hz), 3.24 (Hβ, J = 14 and

Table 1. Crystal Data and Structure Refinement of **1A·HCl**, **1B**, **1C**, and **2**

	1A·HCl·0.25H$_2$O	1B·H$_2$O	1C·2H$_2$O	2·3H$_2$O
formula	C$_9$H$_{12.5}$ClN$_2$O$_{7.25}$ReS	C$_9$H$_{13}$N$_2$O$_8$ReS	C$_9$H$_{15}$N$_2$O$_9$ReS	C$_{10}$H$_{19}$N$_2$O$_{10}$ReS
fw	518.43	495.47	513.49	545.53
space group	P$\bar{1}$	P$\bar{1}$	P2$_1$/c	P2$_1$2$_1$2$_1$
a (Å)	10.8361(9)	8.0524(3)	8.6594(8)	9.2513(5)
b (Å)	11.5484(10)	8.5267(3)	19.5630(18)	11.0612(6)
c (Å)	13.0041 (11)	10.9700(4)	8.9757(8)	16.2289(9)
α (deg)	111.002(2)	77.872(2)	90	90
β (deg)	97.221(2)	78.388(2)	104.032(2)	90
γ (deg)	91.780(2)	73.174(2)	90	90
V (Å^3)	1502.1(2)	696.88(4)	1475.1(2)	1660.71(16)
Z	4	2	4	4
T (K)	100(2)	173(2)	100(2)	100(2)
λ (Å)	0.71073	1.54178	0.71073	0.71073
d$_{calcd}$ (g cm^{-3})	2.290	2.361	2.312	2.182
μ (mm^{-1})	8.441	18.874	8.427	7.496
F (000)	984	472	984	1056
R [I > 2σ(I)]				
R$_1$[a]	0.0446	0.0304	0.0348	0.0254
wR$_2$[b]	0.0968	0.0878	0.0761	0.0587
R (all data)				
R$_1$[a]	0.0567	0.0329	0.0389	0.0260
wR$_2$[b]	0.1015	0.0894	0.0776	0.0590

[a] $R_1 = \sum ||F_o| - |F_c||/\sum |F_o|$. [b] $_wR_2 = [\sum (w(F_o^2 - F_c^2)^2)/[\sum (w(F_o^2)^2)]^{1/2}$.

Table 2. Selected Bond Angles (deg) and Bond Distances (Å) of **1A·HCl**, **1B**, **1C**, and **2**

	1A·HCl[a]		1B	1C	2
N−Re−S	N(1)−Re(1)−S(1) 79.74(12)	N(1B)−Re(1B)−S(1B) 81.29(12)	N(1)−Re(1)−S(1) 80.01(18)	N(1)−Re(1)−S(1) 80.85(9)	N(1)−Re(1)−S(1) 87.41(9)
	N(2)−Re(1)−S(1) 81.09(12)	N(2B)−Re(1B)−S(1B) 79.94(12)	N(2)−Re(1)−S(1) 81.10(19)	N(2)−Re(1)−S(1) 81.49(9)	N(2)−Re(1)−S(1) 80.49(8)
Re−N	Re(1)−N(1) 2.200(4)	Re(1B)−N(1B) 2.225(4)	Re(1)−N(1) 2.212(6)	Re(1)−N(1) 2.229(3)	Re(1)−N(1) 2.249(3)
	Re(1)−N(2) 2.237(5)	Re(1B)−N(2B) 2.204(4)	Re(1)−N(2) 2.236(7)	Re(1)−N(2) 2.215(3)	Re(1)−N(2) 2.214(3)
Re−S	Re(1)−S(1) 2.4664(14)	Re(1B)−S(1B) 2.4592(14)	Re(1)−S(1) 2.472(2)	Re(1)−S(1) 2.4438(10)	Re(1)−S(1) 2.4555(8)

[a] Atom numbers ending with B belong to cation **b**.

6), and 3.09 ppm (Hβ, J = 14 and 5 Hz) are tentatively assigned to the alanyl unit derived from cysteine because there is no evidence of further coupling that might be expected from the Hγ protons of the residue derived from homocysteine.

Crystal Structure Analysis. All products described above were initially isolated as neutral complexes. To obtain crystals suitable for X-ray crystallography, these complexes were dissolved in water by adding NaOH. After adjustment of the pH to ~3 with HCl, the solutions were left at ambient temperature. **1B**, **1C**, and **2** crystallized as neutral complexes with one carboxyl group protonated. However, **1A** crystallized as the hydrochloride (**1A·HCl**) with both carboxyl groups protonated. Crystals were coated with Paratone N oil, suspended in a small fiber loop, and placed in a cooled nitrogen gas stream on a Bruker D8 SMART APEX CCD sealed tube diffractometer with graphite monochromated Mo Kα radiation for **1A·HCl**, **1C**, and **2** and Cu Kα radiation for **1B**. Data were obtained by using a series of combinations of phi and omega scans with 10 s frame exposures and 0.3° frame widths. Data collection, indexing, and initial cell refinements were all carried out by using SMART software (version 5.624 for **1A·HCl**, **1C**, and **2** and version 5.625 for **1B**).[54] SAINT software was used for frame integration and final cell refinements (version 6.02 for **1A·HCl**, **1C**, and **2** and version 6.36A for **1B**).[55] SADABS software was used for absorption corrections (version 2.03 for **1A·HCl**, **1C**, and **2** and version 2.08 for **1B**).[56]

The structures of the complexes were solved by direct methods and difference Fourier techniques (SHELXTL, V5.10 used for **1A·** HCl, **1C**, and **2** and version 6.12 used for **1B**).[57] Hydrogen atoms were located in a difference Fourier map and were included in the final cycles of least-squares with isotropic U$_{jj}$'s related to the atoms ridden upon. All non-hydrogen atoms were refined anisotropically. Scattering factors and anomalous dispersion corrections were taken from the *International Tables for X-ray Crystallography*.[58] Structure solution, refinement, graphics, and generation of publication materials were performed by using SHELXTL software as above. Crystallographic details for all complexes are presented in Table 1; selected bond distances and angles appear in Table 2.

Results

In the complexes studied here, the Re(I) center and the uncharged chelate ring fragments (lacking the carboxyl groups) that create the N$_2$S coordination environment have a net positive charge. Thus, depending on the protonation state of the two uncoordinated carboxyl groups, each complex

(54) *SMART, versions 5.624 and 5.625*; Bruker AXS, Inc.: 5465 East Cheryl Parkway, Madison, WI 53711-5373, 2002.
(55) *SAINT, versions 6.02, 6.36A*; Bruker AXS, Inc.: 5465 East Cheryl Parkway, Madison, WI 53711-5373; 2002.
(56) Sheldrick, G. *SADABS*; University of Gottingen: 1996.
(57) *SHELXTL, versions 5.10, 6.12*; Bruker AXS, Inc.: 5465 East Cheryl Parkway, Madison, WI 53711-5373, 1997; 2002.
(58) Wilson, A. J. C. *International Tables for X-ray Crystallography, Volume C*.; Kynoch, Academic Publishers: Dordrecht, 1992; Vol. Tables 6.1.1.4 (pp 500−502) and 4.2.6.8 (pp 219−222).
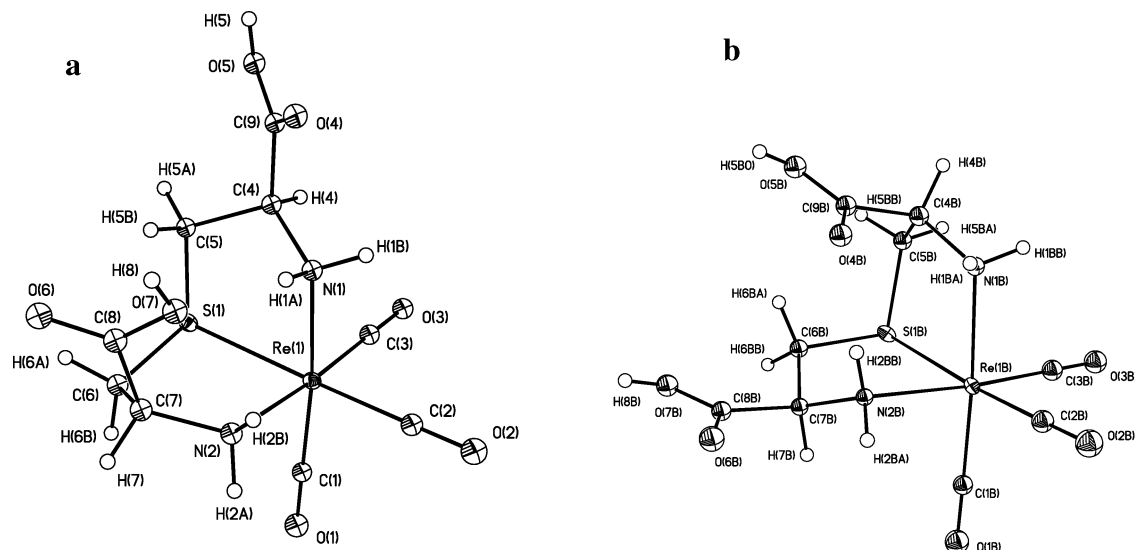
Figure 1. Perspective drawing of the kinetically favored Re(CO)$_3$(*meso*-LANH) isomer crystallized as the cation, [Re(CO)$_3$(*meso*-LANH$_2$)]$^+$, in **1A**·HCl with 50% probability for the thermal ellipsoids. The chloride and water molecules are omitted for clarity. Cation **a** is a pseudoenantiomer of cation **b**.

could possibly exist in three forms (monocation, neutral zwitterion, and monoanion). The term "zwitterion" refers here to the neutral complex having a positive region near the Re(I) and a more remote negatively charged carboxylate group. Products can be obtained as crystals or as precipitates free of free ligand from aqueous solution at pH ∼3 (the optimal pH to precipitate free LANH$_2$ from aqueous solution is ∼6). At around pH 3, **1A** crystallized as a [Re(CO)$_3$(*meso*-LANH$_2$)]Cl salt, in which both carboxyl groups are protonated, whereas crystals of **1B** and **1C** contain the neutral Re(CO)$_3$(LANH) zwitterion. However, elemental analyses indicate that all **1A**, **1B**, and **1C** products obtained under preparative conditions are neutral zwitterions. In preparing NMR solutions, we found that these products were essentially insoluble in D$_2$O, slightly soluble in acidic solution (pH around 1), but rapidly and highly soluble in basic solution (pH > 10).

Crystallographic Studies. X-ray structural analyses confirm that complexes **1A, 1B, 1C,** and **2** are all pseudo-octahedral, with the {Re(CO)$_3$}$^+$ core and the N$_2$S coordination mode of the ligand. The structural parameters within this core are similar and typical for all structures, Table 2. The Re−N bond distances of ∼2.2 Å are consistent with those found in relevant rhenium tricarbonyl complexes.[6] The Re−S bond distances of ∼2.46 Å are close to those of relevant complexes having a ligand with a thioether S anchoring two coordination rings[17,20,59−62] but shorter than Re−S bonds in complexes having a ligand with a thioether S at a terminal position.[6] An interesting feature of the complexes is that the distances between the ligating atoms are close to the values characteristically found for complexes with more typical M−ligating atom bonds of ∼2 Å for N

and ∼2.2 Å for S. Important consequences of these relatively long Re−N and Re−S bonds include the following: more acute bite angles (ligating atom−Re−ligating atom angle); and, because the shorter Re−C bonds lead to more typical ∼90° C−Re−C angles, trans ligating atom−Re−C angles much less than 180°, particularly when the ligating atom anchors two chelate rings.

Compounds Derived from *meso*-LANH$_2$. X-ray crystals of **1A**, obtained from dilute HCl solution, had the composition, **1A**·HCl. The asymmetric unit has two unique [Re(CO)$_3$-(*meso*-LANH$_2$)]$^+$ cations, both containing the neutral *meso*-LANH$_2$ ligand, with both carboxyl groups protonated, but differing in the orientation of the carboxyl groups. As shown in Figure 1, each cation has one chelate ring with a carboxyl group projecting away from the Re (L ring pointing upward in cation **a** and D ring pointing to the left in cation **b**), while the other chelate ring has a carboxyl group projecting toward this first chelate ring. These differences are related to ring pucker and the pseudoenantiomeric relationship of the cations in the solid state, see below.

1C crystallizes with one unique neutral Re(CO)$_3$(*meso*-LANH) molecule in the asymmetric unit (Figure 2). In the solid crystalline state, two complexes in the unit cell are true enantiomers of the other two complexes. In the enantiomer illustrated, the carboxyl group on the D chelate ring of the *meso*-LANH$^-$ ligand is protonated and projects over two CO ligands, whereas the carboxyl group on the L chelate ring is deprotonated and projects away from the Re, as found for one ring in the two cations of **1A**·HCl discussed above. In the other enantiomer, the L chelate ring is protonated, and the D chelate ring is deprotonated. The bond distances and angles involving the Re coordination sphere are very close to those of **1A**·HCl, Table 2.

Compound Derived from *chiral*-LANH$_2$. The X-ray structure of **1B** (Figure 3) has a neutral zwitterionic Re(CO)$_3$-(LANH) form and confirms that the commercial material consists, in part, of a racemic mixture; the molecule illustrated has the L,L-LANH$^-$ ligand (hereafter L-LANH$^-$)

(59) Hoffmann, P.; Steinhoff, A.; Mattes, R. *Z. Naturforsch., B: Chem. Sci.* **1987**, *42*, 867−873.
(60) Heard, P. J.; Tocher, D. A. *J. Organomet. Chem.* **1997**, *549*, 295−304.
(61) Adams, R. D.; Queisser, J. A.; Yamamoto, J. H. *Organometallics* **1996**, *15*, 2489−2495.
(62) Adams, R. D.; Falloon, S. B. *Organometallics* **1995**, *14*, 1748−1755.
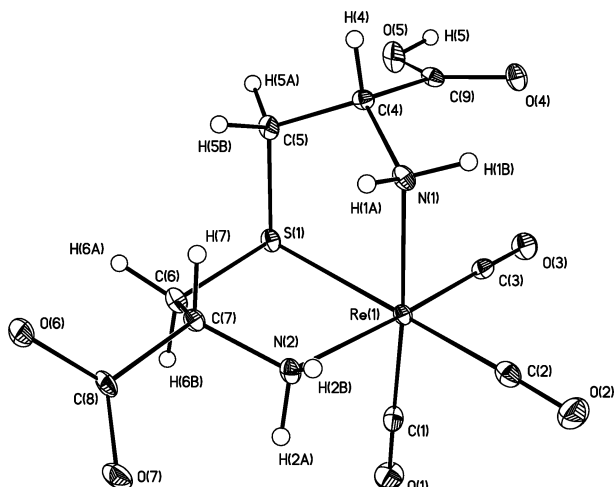
Figure 2. Perspective drawing of the thermodynamically favored Re(CO)₃-(*meso*-LANH) isomer in crystals of **1C** with 50% probability for the thermal ellipsoids. The water molecules are omitted for clarity.
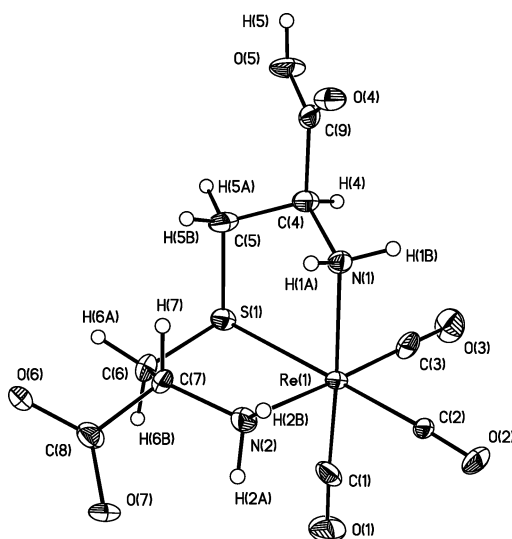

Figure 3. Perspective drawing of the Re(CO)₃(L-LANH) enantiomer in a fully racemic crystal of the Re(CO)₃(*chiral*-LANH) product, **1B**, with 50% probability for the thermal ellipsoids. The water molecule is omitted for clarity.

with both L chelate rings having λ pucker. The chelate ring on the left of **1B** (Figure 3) is very similar to that on the left of **1C** (Figure 2). The chelate ring in the upper part of **1B** (Figure 3) is very similar to that in the upper part of cation **a** of **1A·HCl** (Figure 1). The structure of the **1B** enantiomer shown (Figure 3) thus contains a L-LANH⁻ ligand that can be viewed as a hybrid formed by rings of the meso ligand in the illustrated structures (Figure 1) of the cations of **1A·HCl**. The bond distances and angles of **1B** involving the Re coordination sphere are very close to the corresponding values for **1A·HCl** and **1C**, Table 2.

Compound Derived from L-CSTH₂. The stoichiometric reaction of CSTH₂ with [Re(CO)₃(H₂O)₃]OTf at pH 8 and 75 °C produced **2**. Elemental analysis, NMR spectra, and X-ray crystallographic determination all show that at pH 3 pure **2** crystallizes as Re(CO)₃(CSTH), i.e., in the neutral zwitterionic form, as found for **1B** and **1C**. HPLC indicates that two other minor products are formed; these were not abundant enough to afford sufficient material for character-
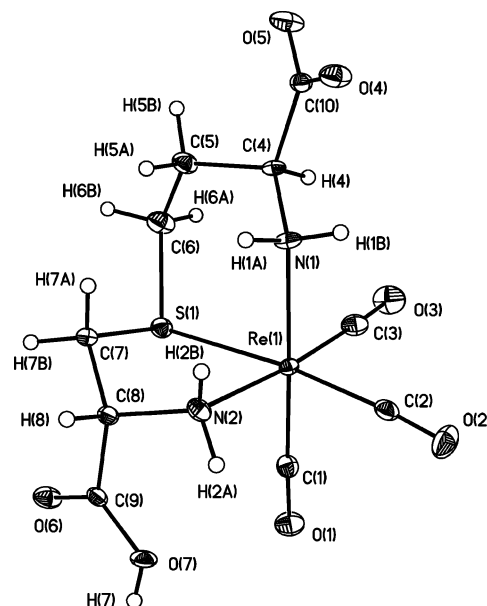

Figure 4. Perspective drawing of Re(CO)₃(CSTH) in **2** with 50% probability for the thermal ellipsoids. The water molecules are omitted for clarity.

ization, but their HPLC retention times compared to that of **2** (10.2 min) suggest that one minor product is the N₂S isomer (11.7 min) and the other is an NOS isomer (6.9 min).

The crystal of **2** contains the complex in the neutral zwitterionic form, and the Flack parameter is 0.019(7), so the absolute configuration shown in Figure 4 is determined with confidence. The tridentate CSTH⁻ ligand forms five-membered and six-membered chelate rings. The five-membered chelate ring of this favored Re(CO)₃(CSTH) product has the δ pucker, and the carboxyl of this L amino acid projects over two CO ligands in a manner somewhat similar to that of the carboxyl of the D amino acid ring (with a λ pucker) in **1C**, the thermodynamically favored Re(CO)₃-(*meso*-LANH) isomer. The Re–N and Re–S bond distances are typical, Table 2.

LANH₂. The biosynthesis of lanthionine derivatives involves Michael addition of cysteine to dehydroalanine,[63] but we found that the chemical synthesis of the excellent lanthionine ligands can be problematic. An early synthetic strategy for LANH₂ involves nucleophilic substitution of chloroalanine by L-cysteine.[41] However, the required strongly basic conditions cause a β-elimination reaction, followed by a Michael addition of the thiolate anion, to give a mixture of diastereoisomers that are not easily separated. Another strategy, involving sulfur extrusion from variously protected L-cystines, was reported to lead to the corresponding mono-sulfides without racemization.[53] We used the latter route to prepare LANH₂. Desulfurization of the *N,N′*-bis(trifluoro-acetyl)-L-cystine dimethyl ester by tris(diethylamino)phos-phine afforded the corresponding lanthionine derivative in high yield, as described in the literature.[53] Deprotection of this lanthionine derivative with 1.0 M NaOH was reported to give L-lanthionine.[53] However, our attempts to reproduce

(63) Okeley, N. M.; Paul, M.; Stasser, J. P.; Blackburn, N.; van der Donk, W. A. *Biochemistry* **2003**, *42*, 13613–13624.

this preparation afforded lower yields than those reported, and the product was predominantly the meso ligand (based on subsequent structural characterization of **1A·HCl** and **1C**). Although the formation of the meso product conflicts with the literature, the result is not surprising because racemization of the α-carbon during the alkaline hydrolysis of the lanthionine ester derivative might be expected. Alternatively, desulfurization of N,N'-(*tert*-butoxycarbonyl)-L-cystine dimethyl ester by tris(diethylamino)phosphine and subsequent deprotection of N-protecting groups by CF_3CO_2H, followed by very mild alkaline hydrolysis (pH between 10.5 and 11.5), gave predominantly chiral LANH₂ material. Because the LANH₂ isomers are neither easily distinguished by spectroscopic methods nor easily separated, we relied on the assessment of the products obtained from their reaction with [Re(CO)₃(H₂O)₃]OTf to determine the relative amount of meso and chiral isomers in a given LANH₂ batch.

Reaction of LANH₂. HPLC traces (Supporting Information) indicate that the reaction of [Re(CO)₃(H₂O)₃]OTf (pH 8, 75 °C, 1 h) with commercial LANH₂ gave comparable amounts of **1A** and **1B** but with predominantly D,L-LANH₂ gave mainly **1B** and with predominantly *meso*-LANH₂ gave mainly **1A**. From the latter preparation, **1A** precipitates from aqueous solution around pH 3 (at room temperature) as the neutral Re(CO)₃(*meso*-LANH) zwitterion. **1A** is kinetically favored and was observed to convert into the thermodynamically favored Re(CO)₃(*meso*-LANH) isomer, **1C**, at pH 8 under reflux conditions (Supporting Information). After 4 h, equal amounts of **1A** and **1C** were found by HPLC; after 6 h the ratio of **1A**:**1C** reached 1:2 and did not change with time.

When the synthetic procedure utilized the mainly L-LANH₂ ligand prepared as above, replacing the predominantly *meso*-LANH₂ starting material, the reaction with [Re(CO)₃(H₂O)₃]-OTf (pH 8, 75 °C, 1 h) afforded a product with **1B** as the major HPLC peak. Because our procedures do not allow us to determine the relative amount of L-LANH₂ and D-LANH₂, we refer to the **1B** product as Re(CO)₃(*chiral*-LANH). To examine if the fully deprotonated coordinated *chiral*-LAN²⁻ ligand undergoes isomerization to the coordinated *meso*-LAN²⁻ ligand as apparently happens with uncoordinated *chiral*-LAN²⁻, the behavior of **1B** under alkaline conditions at ambient temperature was investigated by means of ¹H NMR spectroscopy. At pH 11, ¹H NMR experiments indicated that **1B** remained unchanged in D₂O for up to 5 days. The absence of **1A** or **1C** suggests no isomerization of the coordinated *chiral*-LAN²⁻. In contrast, free *chiral*-LANH₂ isolated from a preparation at pH 11 contained a small amount of *meso*-LANH₂. The absence of Hα exchange of coordinated *chiral*-LAN²⁻ in D₂O at high pH in **1B** may be attributed to steric hindrance by the {Re(CO)₃}⁺ core to the approach of base to one Hα and to the proximity of the other Hα to the negative carboxyl group. Likewise, there was no indication of the presence of **1B** when samples of **1A** or **1C** were subjected to pH 11 conditions.

NMR Spectroscopic Properties. Compounds Derived from *meso*-LANH₂. The ¹H NMR spectrum of each Re-(CO)₃(*meso*-LANH) isomer (**1A** and **1C**) has one set of
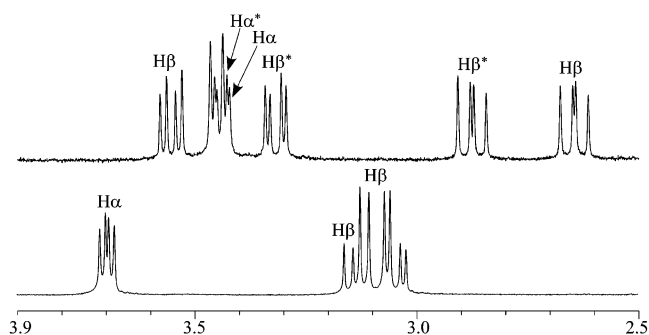

Figure 5. NMR spectrum (2.5−3.9 ppm) of Re(CO)₃(*chiral*-LANH) (**1B**) (top) and of the thermodynamically favored Re(CO)₃(*meso*-LANH) isomer (**1C**) (bottom) in D₂O/NaOD, pH ∼ 11. For **1B**, the asterisk distinguishes the signals of one alanyl residue from the other. The two largest peaks of the overlapped Hα/Hα* signals are from both signals, and the two smallest and two medium-sized peaks are from the Hα and Hα* signals, respectively.

alanyl ¹H NMR signals consisting of one doublet of doublets signal for Hα and two doublet of doublets for Hβ. This result, illustrated for the thermodynamically favored isomer **1C** in Figure 5, indicates that the two alanyl residues are magnetically equivalent on the NMR time scale. After discussing the **1B** spectra obtained, we will analyze these simple spectra further.

Compound Derived from *chiral*-LANH₂. In contrast to **1A** and **1C**, the two alanyl residues are not magnetically equivalent in the Re(CO)₃(*chiral*-LANH) isomer, **1B**. Because of overlap issues and some unusual shifts, ¹H NMR spectra of **1B** were recorded under various conditions. In D₂O at pH 11 (Figure 5), coupling constants observed in 1D ¹H NMR experiments allowed assignments of signals at 3.46 (Hα, $J = 11.4$ and 5.4 Hz), 3.56 (Hβ, $J = 13.8$ and 5.4 Hz), and 2.65 ppm (Hβ, 13.8 and 11.4 Hz) to one alanyl residue and signals at 3.46 (Hα, $J = 10.8$ and 4.2 Hz), 3.32 (Hβ, 14.4 and 4.2 Hz), and 2.88 (Hβ, 14.4 and 10.8 Hz) ppm to the other alanyl residue. The two Hα signals overlap (Figure 5), but the signal pattern is consistent with a simulated signal pattern based on calculations using the indicated coupling constants. **1B** can be made slightly soluble in D₂O by adding DCl. 1D and COSY NMR spectra of **1B** were recorded at pH 1 (uncorrected). Four well-resolved NH signals were observed, each integrating for one proton. In addition, four Hβ signals for the two CH₂ groups were well separated. Because two Hα signals are partially overlapped (3.68−3.71 ppm), the COSY correlations of Hα could not be resolved. However, we could obtain important correlations within each CH₂: 3.79 and 2.65 ppm for one CH₂ and 3.64 and 2.91 ppm for the other CH₂. The unusual conclusion from coupling data that one Hβ signal is downfield to the Hα signals is thus confirmed. COSY cross-peaks indicate that signals at 6.10 and 4.06 ppm belong to one NH₂ group and those at 5.32 and 5.21 ppm belong to the other NH₂ group.

This pattern for **1B** in DCl (the difference in chemical shifts for two NH signals for one NH₂ group is greater than for the other NH₂ group) appeared to be related to our previous findings with Re(CO)₃(CCMH) (CCMH₂ = *S*-carboxymethyl-L-cysteine) isomers in DMSO-d_6.[6] In a COSY experiment on **1B** in DMSO-d_6, the multiplet at 3.22 ppm

(Hα) correlates with signals at 5.44 and 5.10 ppm; these two signals are assigned to the NH protons in the same alanyl residue, a result confirmed by a COSY cross-peak connecting the two NH signals. The same Hα signal also correlates with signals at 2.57 and 3.56 ppm, assigned to the two Hβ protons in this alanyl residue. The signals of the other alanyl residue are easily assigned by correlations of the Hα signal at 3.00 ppm with NH signals at 6.19 and 3.92 ppm (in turn connected by a COSY cross-peak) and with Hβ signals at 2.25 and 3.64 ppm.

It is important to note that spectra of **1B** recorded in both D$_2$O (Figure 5) and DMSO-d_6 show that one alanyl residue has greater differences in chemical shifts between the two NH signals and the two Hβ signals than does the other alanyl residue. This pattern, which is particularly evident for the NH signals, is unlikely to be a through-bond inductive effect because the electronic effect of the symmetric Re(CO)$_3$ group should be similar for both amino groups. Also, the pattern is found for three solvent situations (carboxyl groups in the LAN ligand bearing either no protons at pH 11, one proton in DMSO-d_6, or two protons at pH 1) that are expected to alter an inductive effect. This pattern undoubtedly arises from a through-space effect, reflecting a different structural relationship to the remainder of the complex of the protons of one alanyl residue compared to those of the other residue.

As mentioned, we observed in spectra for Re(CO)$_3$-(CCMH) the same kinds of ^{1}H NMR shift relationships noted here in spectra of **1B**.[6] Because CCMH$^-$ has a chiral carbon and because sulfur has two lone pairs of electrons, Re(CO)$_3$-(CCMH) exists as two diastereoisomers, which were fully characterized. One isomer is kinetically favored, while the other isomer is thermodynamically favored. Both isomers have the same coordination atoms, and CCMH$^-$ acts as a tridentate monoanionic ligand through the amino, the thioether, and the S-carboxymethyl carboxyl groups. This coordination pattern is very relevant to the Re analogues reported here because the carboxyl group is not coordinated and is attached to an NS-bound alanyl chelate ring. Thus the alanyl units are very similar (CCMH$^-$ vs LANH$^-$), including the presence of a thioether donor. Furthermore, as found for **1B**, the Hα signal is relatively upfield for the Re-(CO)$_3$(CCMH) isomers. NMR spectra (in DMSO-d_6) show that the differences in chemical shifts for the two Hβ signals and particularly for the two NH signals of the alanyl residue for the kinetically favored Re(CO)$_3$(CCMH) isomer are clearly greater than these differences for the thermodynamically favored isomer.[6]

In order to describe signal assignments, the protons are defined according to the atom-labeling scheme used for the molecular structure of **1B** (Figure 3). We assigned the NH signals to an alanyl moiety of **1B** by comparison of the **1B** spectrum with those of the Re(CO)$_3$(CCMH) isomers.[6] One NH (trans to Hα) of **1B** is distinctively positioned. The N(1)−H(1A) and metal carbonyl C(3)−O(3) bonds lie almost in the same plane, and the N(1)−H(1A) bond is trans to the C(3)−O(3) bond; similar arrangements were found in the kinetically favored Re(CO)$_3$(CCMH) isomer. In contrast, the N(2)−H(2A) and carbonyl C(1)−O(1) bonds lie in the same

plane, but the N(2)−H(2A) bond is cis to the C(1)−O(1) bond; similar arrangements were found in the thermodynamically favored Re(CO)$_3$(CCMH) isomer. Furthermore, by taking advantage of the relationship between coupling constants and torsion angles, all signals of **1B** in DMSO-d_6 were tentatively assigned as follows (for atom numbering, see Figure 3): for one alanyl residue (ppm), 3.00 [H(4)], 6.19 [H(1B)], 3.92 [H(1A)], 3.64 [H(5A)], 2.25 [H(5B)]; and for the other residue (ppm), 3.22 [H(7)], 5.44 [H(2B)], 5.10 [H(2A)], 3.56 [H(6A)], 2.57 [H(6B)]. Signals of the NH and the Hβ trans to Hα are both upfield relative to these signals for the respective protons cis to Hα.

Discussion

α-Amino acids bearing sulfur donors generally act as bidentate ligands, as exemplified by a number of metal complexes that have a bidentate methionine or S-methyl-cysteine coordinated through N, O or N, S donor atoms.[64−69] In contrast, MECYS$^-$ and PRCYS$^-$ are tridentate in fac-Re(CO)$_3$(NOS) complexes (MECYSH = S-methyl-L-cysteine, PRCYSH = S-propyl-L-cysteine).[6] However, the S-dipeptide ligands in the present study favor the N$_2$S tridentate chelation mode in all four new complexes because, as explained in the Introduction, oxygen coordination would lead to unfavorably larger chelate rings.

As mentioned in the Introduction, the unique feature of the S-dipeptides employed in the current study is that the amino acids are not linked by the classical peptide amide group but by a thioether group. These two types of groups differ in several ways. Obviously when an amide binds via the N atom, the amide must deprotonate. Thus it binds as a negative amido group, whereas the thioether group is neutral. The amido group is a strong electron donor and is a very strong field ligand. The thioether group, on the other hand, is a weaker donor and could utilize some π-bond character when forming bonds to low-valent metal centers such as Re-(I). The most important difference between amido and thioether donors, however, is the difference in the relative disposition of the two chelate rings that incorporate these donors. The amido group enforces coplanarity on these rings, whereas the thioether group prevents coplanarity, thus favoring the facial coordination geometry needed for the {^{99m}Tc(CO)$_3$}$^+$ core.

Because it has C$_2$ symmetry, upon coordination chiral-LANH$_2$ can form only one N$_2$S tridentately ligated geometric isomer (**1B**), regardless of which of the two available lone pairs on sulfur binds to the Re(I). In contrast, the most interesting and informative results involve the two isomers

(64) Brand, U.; Rombach, M.; Seebacher, J.; Vahrenkamp, H. *Inorg. Chem.* **2001**, *40*, 6151−6157.
(65) Yamanari, K.; Fuyuhiro, A. *Bull. Chem. Soc. Jpn.* **1995**, *68*, 2543−2550.
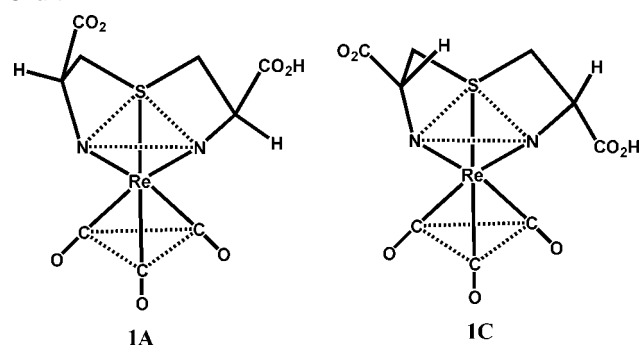(66) de Meester, P.; Hodgson, D. J. *J. Am. Chem. Soc.* **1977**, *99*, 6884−6889.
(67) Gainsford, G. J.; Jackson, W. G.; Sargeson, A. M. *J. Chem. Soc., Chem. Commun.* **1979**, 802−803.
(68) Caubet, A.; Moreno, V.; Molins, E.; Miravitlles, C. *J. Inorg. Biochem.* **1992**, *48*, 135−152.
(69) Kovalev, Y. G.; Ioganson, A. A. *Zh. Obshch. Khim.* **1987**, *57*, 1939−1943.

Chart 2

1A   1C

derived from the *meso*-LANH$_2$ ligand. The free *meso*-LANH$_2$ ligand possesses mirror symmetry, but the sulfur is a prochiral center; this combination opens the possibility of the formation of two Re(CO)$_3$(*meso*-LANH) diastereoisomers (**1A** and **1C**), depending upon which lone pair coordinates to the {Re(CO)$_3$}$^+$ core (see Chart 2, also see X-ray crystal structure discussion). Another way to comprehend these possibilities is to visualize the {Re(CO)$_3$}$^+$ unit adding from opposite directions to the *meso*-LANH$_2$ ligand.

As illustrated for the lanthionine complexes in Chart 2, the β carbons (attached to sulfur) project upward, away from the {Re(CO)$_3$}$^+$ unit. The X-ray structures reveal that the backbone structure of the chelate rings, N−C−C−S−C−C−N, is rather similar in all isomers (**1A**, **1B**, **1C**). However, the torsion angles in one chelate ring differ from those in the other chelate ring in such a way that the puckers of the two chelate rings have the same chirality, δ or λ. In all cases, regardless of the configuration of the α carbons (meso vs chiral LAN^{2-}) of the ligand or of the isomer (**1A** vs **1C**), the similar chirality of the pucker of the two chelate rings results in the α carbon of one chelate ring projecting toward the other chelate ring, and the α carbon of this other ring projecting away from the first (partner) chelate ring.

We noted above that in **1B**, the shifts of the protons in the two chelate rings have very different patterns. These rings cannot interchange. Because one ring of **1B** has a structure very similar to that of the alanyl chelate ring in the kinetically favored Re(CO)$_3$(CCMH) isomer, and also the shifts of the pair of alanyl NH signals with the well-separated NH signals are very similar to the shifts of the NH signals of this CCMH isomer, we tentatively assign this set of alanyl signals to the **1B** chelate ring which is similar in structure to the ring in this Re(CO)$_3$(CCMH) isomer. This chelate ring is in the upper part of **1B** in Figure 3; we call this ring type the "NH trans to CO" ring. Furthermore, we note that the NH signals for this chelate ring of **1B** (∼4 and ∼6 ppm) have an average shift of ∼5 ppm, a value very similar to the average for the NH signals of the other **1B** chelate ring (which we call the "normal" ring) and to the averages for the NH signals found for **1A** and **1C**. Because of the limited data available at this time, we cannot offer a definitive explanation as to why the "NH trans to CO" chelate ring has one NH signal upfield by ∼1 ppm and the other NH signal downfield by ∼1 ppm from the normal NH shift. Work in progress has identified other chelate complexes with unusual NH shifts, and eventually we may have a better understanding of the factors

leading to shielding and deshielding of NH signals. At this time, we believe the effects are through space. An inductive effect of the Re(I) is unlikely to be very different for the two amino groups because of the symmetric nature of the Re(CO)$_3$ moiety. Also, an inductive effect is likely to cause both signals of a given group to shift in a similar manner. However the interesting signals for the amino group differ by about 2 ppm. The cause of the large shift difference is therefore undoubtedly through space. The upfield/downfield nature of the effect suggests an anisotropy.

Above we stressed the fact that the NMR spectra of **1A** and **1C** indicate a time-averaged mirror symmetry possible for these isomeric Re(CO)$_3$(*meso*-LANH) complexes. The X-ray structures reveal that the process leading to this time averaging is more than just an exchange of the site of carboxyl group protonation. The data indicate that the ring structures are undoubtedly interchanging in a coordinated fashion, with rotation occurring about the S−C, C−C, and C−N bonds in both rings. This analysis is best understood by examining the X-ray structure of **1A**·HCl. The unit cell has four cations. Each of the two cations illustrated in Figure 1 has an enantiomer, not shown. In the solid, the detailed geometry of one pair of enantiomers is slightly different from that of the other pair. The two cations illustrated have a pseudoenantiomeric relationship because each is from a different enantiomeric pair. In cation **a** (Figure 1), with both chelate rings having λ pucker, the carboxyl on the left chelate ring projects toward the other chelate ring, whereas the carboxyl on the other ring projects away from the left chelate ring and also away from the Re. Compared to cation **a**, the directions of carboxyl projection found for cation **b** (Figure 1) are interchanged between the rings, both of which have δ pucker. In solution and in the absence of solid-state effects, the two conformers (represented by cation **a** and cation **b**) will be true enantiomers. A fast fluxional conformational interchange between enantiomeric conformers, one with δ,δ pucker and one with λ,λ pucker, is the type of motion that explains the apparent symmetry reflected in the NMR data. A similar argument can be made for **1C**. Although Figure 2 shows the structure of only one of the four molecules of **1C** in the unit cell, one of the other three has exactly the same structure, and the other two are true enantiomers of these two. As such, whereas the structure shown has the λ,λ pucker, the enantiomer has the δ,δ pucker. Rapid time averaging on the NMR time scale leads to the simple NMR spectrum observed.

The shifts of the chelate ring protons, especially the NH protons, provide further support for such fluxional behavior. In both **1A** and **1C** one of the two chelate rings has the "NH trans to CO" structure found for one of the rings in **1B**. If no interchange occurred, we would expect to find well-separated NH signals, as found for **1B**. However, the interchange process we envision for **1A** and **1C** should average the NH shifts, explaining the absence of well-separated NH signals for **1A** and **1C**.

As mentioned, **1A** is the kinetically favored Re(CO)$_3$-(*meso*-LANH) isomer, and **1C** is the thermodynamically favored isomer. In **1A**, although the two carboxyl groups

are positioned somewhat differently, both are above the plane defined by N_2S; i.e., the two carboxyl groups are positioned anti to the $\{Re(CO)_3\}^+$ core and during the fluxional process the Re–C (carboxyl) distance varies between ~4 and 4.5 Å. In contrast, in **1C** one carboxyl group is below the plane defined by N_2S; the Re–C (carboxyl) distance is ~3.6 Å, and this carboxyl group is thus positioned syn to the $\{Re(CO)_3\}^+$ core. Under the pH conditions used to equilibrate **1A** and **1C**, the carboxyl groups are deprotonated, and one possible explanation for the slightly higher stability of **1C** over **1A** is an electrostatic attraction of the carboxyl group for the Re(I) center. Likewise, during the reaction forming the meso-LAN complex isomers, this syn positioning could cause the negative carboxyl group to hinder the approach by the species derived from $[Re(CO)_3(H_2O)_3]^+$. At the pH of the preparative reactions (~pH 8), the Re synthon most likely carries a negative charge, and formation of **1C** could be impeded. Also, the syn positioning of the carboxyl group could sterically hinder formation of **1C**. These types of factors could explain why **1A** is kinetically favored and **1C** is thermodynamically favored.

It is worth noting that radiolabeling of predominantly *meso*-LANH$_2$ with $[^{99m}Tc(CO)_3(H_2O)_3]^+$ (pH 9, 70 °C, 30 min) yielded a peak corresponding to **1C** as the major product (Supporting Information). This result indicates that the **1A** to **1C** conversion process is much easier in the ^{99m}Tc complex than in the Re complex, as expected in a comparison of second- and third-row transition elements. This kinetic difference in no way diminishes the utility of Re analogues for assessing the likely structure of ^{99m}Tc agents.

Summary and Conclusions

1A–**C** and **2** are the first well-characterized coordination complexes with lanthionine or cystathionine. Re(CO)$_3$-(LANH) isomers favor N_2S coordination and leave dangling carboxyl groups, consistent with the high renal clearance of the ^{99m}Tc lanthionine agents. All LAN complexes have similar unsymmetric N–C–C–S–C–C–N geometry with both chelate rings having the same pucker chirality, i.e., either λ,λ pucker or δ,δ pucker. For Re(CO)$_3$(*meso*-LANH) isomers, the presence of rings having the same pucker leads to two conformational enantiomers which interchange rapidly, leading to simple NMR spectra. For Re(CO)$_3$(*chiral*-LANH), in a given molecule, the α carbons have the same chirality, but the preference for the rings to have the same pucker leads to two relatively different chelate rings within each true enantiomer. These enantiomers have the same NMR spec-

trum, but the chelate rings are not magnetically equivalent. In some cases, the NH signals have unusual shifts. As more studies are performed on the important class of compounds with coordinated amino groups and a metal tricarbonyl core, the exact factors causing these unusual shifts might be understood. The weight of the evidence suggests that inductive (electronic through-bond) effects are not responsible but that the effect may be caused by anisotropy, possibly of the Re(I) center.

The synthesis and complete characterization of rhenium complexes was motivated by the expectation that the results would provide information that will facilitate design and development of ^{99m}Tc tricarbonyl radiopharmaceuticals. Parallel studies of Re and ^{99m}Tc agents are expected not only to facilitate ^{99m}Tc tracer design but also to spur the development of therapeutic β-emitting ^{186}Re- and ^{188}Re-based radiopharmaceuticals. Moreover, the uncoordinated carboxyl groups in these complexes can be exploited for conjugation of the other peptides and proteins, making this class of complexes a useful platform for the development of radiopharmaceuticals other than renal imaging agents. A finding in the current work quite relevant to radiopharmaceuticals is the existence of short-lived enantiomers in the case of a meso ligand lacking overall chirality. The dynamic processes discussed above give a time-averaged form, and, for example, only one peak is found by HPLC, as expected. On the other hand, the biological target (in the present case the renal transporter) could well select between these enantiomers. This relationship should be kept in mind during the design of ^{99m}Tc(CO)$_3$ radiopharmaceuticals.

Supporting Information Available: X-ray crystallographic data for compounds **1A**–**C** and **2** in CIF format and HPLC chromatograms of lanthionine complexes with the $\{M(CO)_3\}^+$ core (M = ^{99m}Tc, Re). This material is available free of charge via the Internet at http://pubs.acs.org.

IC0619299